Electrical Power and Energy Systems 147 (2023) 108887

Contents lists available at ScienceDirect

International Journal of Electrical Power and Energy Systems

journal homepage: www.elsevier.com/locate/ijepes

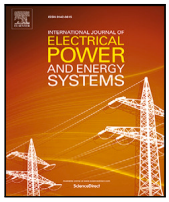

A novel two-stage TSO–DSO coordination approach for managing congestion and voltages

Muhammad Usman, Mohammad Iman Alizadeh, Florin Capitanescu *, Iason-Iraklis Avramidis, André Guimaraes Madureira

Luxembourg Institute of Science and Technology (LIST), Environmental Research and Innovation (ERIN) Department, 41-rue du Brill, L-4422 Belvalux, Luxembourg

ARTICLE INFO

Keywords:
Congestion management
Flexibility
N-1 security
Optimal power flow
TSO–DSO coordination
Voltage control

ABSTRACT

This paper proposes a novel approach to TSO–DSO coordination in day-ahead operation planning for the procurement of ancillary services (AS) such as congestion management and voltage control. The approach overcomes two major issues hindering practical applicability of existing TSO–DSO coordination mechanisms, namely the computational complexity due to the large number of times the TSO and DSO problems are resolved as well as the inability to map analytically the cost and amount of flexibility at DSO level into TSO problem. To this end, a two-fold novelty of our approach consists of the decomposition of the overall AS problem into two sequential stages, which seek the procurement of: (i) "active power related" AS (i.e., for congestion management) and then (ii) the "reactive power related" AS (i.e., for voltage support), respectively as well as a fast approximation of the cost of aggregated active and reactive power flexibilities of active distribution systems (ADSs). Unlike existing mechanisms, the proposed approach considers real-world challenging aspects such as the N-1 security at TSO level and operation uncertainties at both TSO and DSO levels. Accordingly, the approach relies on tailored versions of stochastic multi-period AC security-constrained optimal power flow (S-MP-SCOPF) at TSO level and stochastic multi-period AC optimal power flow (S-MP-OPF) at DSO level, which are formulated as non-linear programming (NLP) problems. The importance and performance of the proposed approach are illustrated on a power system connecting a 60-bus transmission system (under 33 N-1 contingencies) with five 34-bus ADSs.

1. Introduction

1.1. Motivation

Decarbonization of power systems worldwide entails an accelerated penetration of variable renewable energy sources (RES), such as wind and solar, in both active distribution systems (ADSs) and transmission system (TS). The variability of RES power production threatens the task of distribution system operators (DSOs) and transmission system operator (TSO) to meet operation limits (e.g., voltage magnitude, branch current). Mitigating such challenges requires power adjustments of RES and additional flexibility options, e.g., electrical energy storage (EES) systems and flexible loads (FLs).

Furthermore, the fact that a huge number of these flexibility sources are located in ADSs, hence not visible or directly controllable by the TSO, has two implications: (i) the operation of TS becomes increasingly dependent on the operation of ADSs and (ii) the TSO controllability of secure operation diminishes (e.g., some dispatchable power plants may be displaced by RES). At the same time, DSO, which in the past (passive distribution network era) was exclusively dependent on the TSO, is generally not self-sufficient in electricity and will still remain heavily dependent on the power supply from the TSO. Consequently, for a cost-effective utilization of flexible resources at system level and avoiding the risk of entire system blackout, that will affect both TSO and DSOs, there is a stringent need to enhance the cooperation between TSO and DSOs. Specifically, the coordination should ensure the DSO-controlled procurement of flexibility by TSO from ADSs, e.g., for ancillary services (AS) such as congestion management and voltage control [1–3]. Accordingly, the topic of coordinating optimal operations of TSO and DSOs has gained momentum, being rightfully perceived as the key enabler for massive integration of RES in power systems.

* Corresponding author.
E-mail address: fcapitanescu@yahoo.com (F. Capitanescu).

https://doi.org/10.1016/j.ijepes.2022.108887
Received 14 June 2022; Received in revised form 8 November 2022; Accepted 4 December 2022
Available online 11 December 2022

Nomenclature

E	Set of electrical energy storages (EES) indexed by e
F	Set of flexible loads (FLs) indexed by f
G	Set of conventional generation units indexed by g
K	Set of operation states indexed by k, including normal operation ($k = 0$) and contingencies ($k \geq 1$)
L	Set of lines indexed by l
N	Set of nodes indexed by n
O	Set of on-load tap changers (OLTCs) indexed by o
R	Set of renewable energy sources (RES) indexed by r
S	Set of uncertainty scenarios indexed by s
T	Set of time periods indexed by t
$\alpha^k_{o,s,t}$	Ratio of OLTC transformer o
$\kappa^k_{o,s,t}$	Auxiliary variable representing the deviation of transformer o ratio from its initial value
$\phi^k_{r,s,t}$	Angle defining RES power factor $\cos(\phi^k_{r,s,t})$
$e^k_{n,s,t}$	Real part of complex voltage $e_{n,s,t}+jf_{n,s,t}$ at bus n
$f^k_{n,s,t}$	Imaginary part of complex voltage at node n
$P^{ch,k/dch,k}_{e,s,t}$	Active power charging/discharging of EES e
$P^{fod,k/fud,k}_{f,s,t}$	Active power over-/under-demand of FL f
$P^k_{g,s,t}$	Active power production of generator g
$P^{c,k}_{n,s,t}$	Active power curtailment of load at node n
$P^{c,k}_{r,s,t}$	Active power curtailment of RES unit r
$P^{TD}_{s,t}/Q^{TD}_{s,t}$	Active/reactive power flow at TSO–DSO interface for active distribution system (ADS) optimization problems (OPs)
P^{TD}_t/Q^{TD}_t	Active/reactive power flow at TSO–DSO interface for transmission system (TS) OPs
$Q^k_{g,s,t}$	Reactive power production of generator g
$Q^{c,k}_{n,s,t}$	Reactive power curtailment of load at node n
$SoC^k_{e,s,t}$	State-of-Charge (SoC) of EES e
ΔP_g	Ramp rate limit of generator g
η^{ch}_e/η^{dch}_e	Charging/discharging efficiency of EES e
$\overline{\phi}_{r,s,t}$	Angle defining the maximum power factor $\cos(\overline{\phi}_{r,s,t})$
$\overline{P}^{TD}/\underline{P}^{TD}$	Active power limits at TSO–DSO interface for ADS OPs
$\overline{P}^{TD}_t/\underline{P}^{TD}_t$	Bounds on active power flow at TSO–DSO interface for TS OPs
$\overline{Q}^{TD}/\underline{Q}^{TD}$	Reactive power limits at TSO–DSO interface for ADS OPs
$\overline{Q}^{TD}_t/\underline{Q}^{TD}_t$	Bounds on reactive power flow at TSO–DSO interface for TS OPs
π_s	Probability of occurrence of scenario s
$\underline{x}/\overline{x}$	Minimum/maximum value of x (e.g., V, SoC, P_g)
$\varphi_{f,s,t}$	Angle defining FL f power factor $\cos(\varphi_{f,s,t})$
c^{flx}_t	Flexibility cost during time period t
c_e	Cost (€/MWh) of usage of EES e
c_{fl}	Cost (€/MWh) of demand flexibility f
c_g	Cost (€/MWh) of power re-dispatch of generator g
c^c_n	Cost (€/MWh) of curtailed load at node n
c_{oltc}	Cost (€) of OLTC transformer operation
$c^{viol}_{p/q/v}$	Cost (€/(MW/MVAr/V)) of active/reactive/voltage shift from defined schedule at TSO–DSO interface
c^c_r	Cost (€/MWh) of curtailed active power of RES r
D	Demand flexibility factor as % of available FL
g_{nm}/b_{nm}	Conductance/susceptance of the branch nm
$P^{ch,rat}_e$	Rated active power charging of EES e
$P^{dch,rat}_e$	Rated active power discharging of EES e
$P^{fd}_{f,s,t}$	Total active power of FL f at bus n
$P^{\star}_{g,t}$	Active power of generator g cleared in energy market
$P^d_{n,t}/Q^d_{n,t}$	Active/reactive power demand at bus n
$P^0_{r,s,t}$	Active power production of RES unit r
P^{TD*}_t/Q^{TD*}_t	Optimum active/reactive power set-point at TSO–DSO interface
V^{TD*}_t	Optimum voltage set-point at TSO–DSO interface

1.2. Related works

The coordination between TSO and DSOs has been the topic of recent research [4–10]. These works look in a system-holistic way (i.e., modeling both TS and ADSs) at minimizing overall system operation cost. They employ various decomposition methods (e.g., hierarchical [5], generalized master–slave splitting method [9], surrogate Lagrange relaxation [10]) *that require a substantial number of iterations, e.g. tens to hundreds [11], between TSO problem and DSOs problems, and are thereby computationally burdensome*. Another shortcoming of these works is that they optimize a single (common) goal for the entire system, i.e., the summation of operation costs of TSO and DSOs, which is inadequate as TSO and DSOs have not only their own cost goals, limited to their jurisdiction, but also do not share them with other entities, and hence compete with each other to minimize their cost. Finally, convex relaxations are often employed (e.g., second order cone programming [4,5,10]) *which do not guarantee returning feasible solutions. The three issues of these works hinder their practical application and are the key motivations of our methodology*.

Another research idea, as a prerequisite to TSO–DSO coordination mechanisms, consists of quantifying the flexibility of ADSs to support TSO procurement of AS. A first class of approaches focuses on either active [12,13] or reactive power [14,15] flexibility at TSO–DSO interface, to tackle specific operation issues (e.g., economic dispatch [12], frequency regulation [13], voltage instability [14] or voltage support [15]).

A broader class of approaches relies on the concept of PQ flexibility charts,[1] generated by the DSO at its interface with the TSO for a given hour of the next day [16–19]. Although PQ charts provide the

[1] The PQ chart of a given ADS (see Fig. 1) is the region in the space of active and reactive power flows at the TSO–DSO interface, which maps all possible power values of flexible resources from that distribution system for which ADS operation constraints are met.

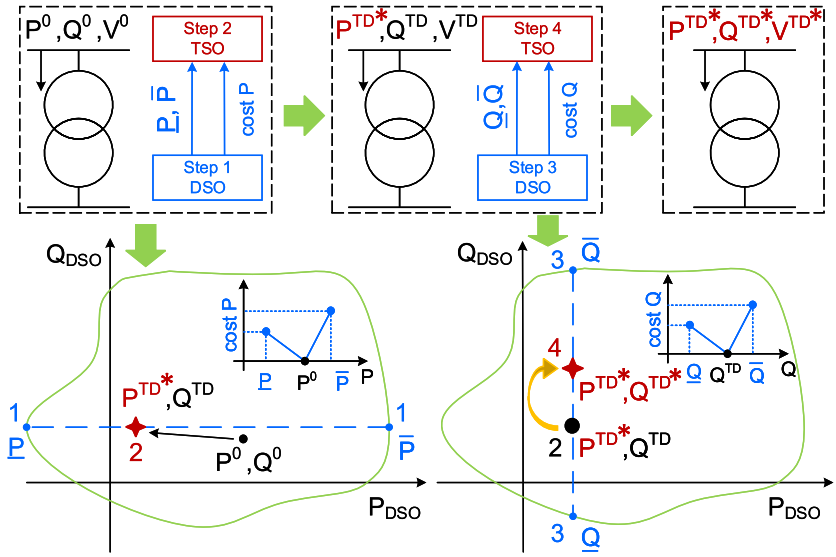

Fig. 1. Conceptual illustration of the proposed AS procurement methodology at a given time step and difference compared to PQ charts.

information about possible flexibility availability in ADSs, computing an accurate approximation of a PQ chart requires large computation effort. Even worse, the key limitation of PQ charts is that they are *only feasibility regions* and *cannot be applied alone to TSO–DSO coordination* because it is not yet known how to map analytically the cost associated to any point in the PQ chart (each cost reflects individual costs of various distributed energy resources employed and it is not known beforehand what point will be selected by the TSO) into a reasonable number of constraints, which can be incorporated in TSO tools to compute flexibility requests at the TSO–DSO interface. *This key limitation of PQ charts is another motivation and rationale for our methodology*. Ref. [20] is the first work proposing an approach that integrates simple PQ chart box constraints at TSO/DSO interface into TSO tools, enabling the latter to solve power balance issue in short-term.

Finally, there are other works in the domain of TSO–DSO coordination that look at the different aspects of TSO–DSO coordination (e.g., markets and pricing for flexibility procurement [21,22] or ICT architectures for data exchange between TSO and DSO [23]). However, these use over-simplified models as regards network operation. For example, [21] focuses on market issues and uses linear DC model without contingencies for TSO problem and second order cone relaxation in DSO problem.

1.3. Paper contributions

The proposed multi-stage TSO–DSO coordination approach circumvents the above issue of mapping the amount of aggregated flexibility to its cost by developing a fast approximation of the cost of flexible active and reactive power flows at TSO–DSO interface (i.e., cost as a function of amount of active/reactive power flows re-dispatch) to be embedded as bids in TSO AS procurement tools. The salient feature of the proposed approach is that the DSO provides *successively* the range of flexible active and reactive powers flows at the TSO–DSO interface along with their costs, which are then embedded in AS markets at TSO level. Consequently, the proposed methodology decomposes the overall problem of joint AS procurement into two sequential stages, which seek the procurement of: (i) "active power related" AS (i.e., for congestion management) and then (ii) the "reactive power related" AS (i.e., for voltage support), respectively. *As compared to existing classical decomposition mechanisms (which may require hundred of iterations), the proposed coordination mechanism requires maximum one iteration between TSO and DSO to remove congestion, and another one to remove voltage issues. Accordingly, it reduces the number of iterations between TSO and DSOs problems to maximum two, one per stage.*

Further motivation and advantages of the proposed sequential procurement of AS and power ranges instead of PQ chart are: (i) in general the control means to relieve congestion (e.g., generators active power) are ineffective to improve voltages while the means to control reactive powers (e.g., generators terminal voltage) are ineffective in relieving congestion, (ii) if congestion and voltage issues do not occur simultaneously in a TS, the approach solves tailored problems of smaller size and hence is faster, and (iii) tremendous reduction of the computation burden as, for each power range, one can compute at least three intermediate points (e.g., the initial point and two extreme points of the range) and derive accordingly a linear function approximating the flexibility cost.

Accordingly, the paper original contributions are as follows:

1. a novel methodology for optimal TSO–DSO coordination in a day-ahead operation framework, which allows both TSO and DSOs to maintain a reliable and cost-effective operation of their networks by procuring AS from the available flexibility options in ADSs;
2. a fast approximation of aggregated active/reactive power flexibility cost of ADS, easy to embed in TSO tools;
3. unlike existing TSO–DSO coordination mechanisms, our approach includes additional computationally challenging features: consideration of *N-1 security* and utilization of *non-linear AC power flow model* in TSO OP, and modeling of *uncertainties* in both TSO and DSO OPs.

Following-up the third contribution, Table 1 clearly highlights that this work is much more detailed in modeling complexity and features than the state-of-the-art; such a detailed (stochasticity, inter-temporal, contingencies, flexibility cost) TSO–DSO coordination model is studied here for the first time.

2. Proposed multi-stage TSO-DSO coordination methodology

The proposed approach assumes the existence of: (i) a local AS market for flexible resources connected at distribution level and (ii) a global market for both flexible resources connected at transmission level and flexibility from ADSs aggregated at each substation interfacing TSO and DSOs. As the topic of TSO–DSO coordination is new, market mechanisms to share flexibility between TSO and DSOs are under investigation [2]; hence, the best way to establish such markets

Table 1
Key features of existing approaches versus this work.

Ref	Flexibility (PQ Flow)		System models		Features			Flexibility cost		TS/ADS	Comparison
	P	Q	TS	ADS	S	MP	N-1	P	Q	size	
[4]	✓	✓	DC	SOCP						3/3	
[5]	✓	✓	SOCP	SOCP						6/336	
[6]			DC	NLP						118/2	
[7]			NLP	NLP	✓					118/69	
[8]	✓		DC	LP						118/33	
[10]	✓	✓	DL	SOCP						118/34	
[11]	✓	✓	NLP	NLP						14/38	
[24]	✓		NLP	NLP		✓	✓	✓		60/34	
[20]	✓	✓	NLP	N/A				✓	✓	60/–	
[12]	✓		N/A	NLP	✓	✓	N/A			–/22	
[13]	✓		N/A	NLP			N/A	✓		–/11	
[14]		✓	N/A	BFS		✓	N/A			–/34	
[15]		✓	N/A	NLP	✓		N/A			–/37	
[25]		✓	N/A	SOCP	✓		N/A			–/77	
[16]	✓	✓	N/A	ICPF			N/A			–/861	
[17]	✓	✓	N/A	NLP		✓	N/A			–/34	
[18]	✓	✓	N/A	LP	✓		N/A			–/33	
[19]	✓	✓	N/A	NLP			N/A			–/33	
This work	✓	✓	NLP	NLP	✓	✓	✓	✓	✓	60/34	

S: stochasticity; **MP**: multi-period; **SOCP**: second-order cone programming; **DL**: dynamic linear; **LP**: linear programming; **BFS**: backward forward sweep; **ICPF**: interval constrained power flow.

is out of our scope. We also assume that energy and reserves markets (e.g., unit commitment) have been cleared before these AS markets and hence, the *grid-unconstrained* market-desired active and reactive power flows between TSO and DSOs are known.

Fig. 1 illustrates conceptually the rationale of the proposed approach when both congestion and voltage issues occur simultaneously, for the sake of simplicity, focusing on one TSO–DSO interface, one time step and ignoring uncertainties. The main outcomes of TSO computation steps are colored in red while DSO's ones in blue. The upper part of the figure shows the sequence in which the common variables of TSO and DSO at the interface (active and reactive power flows and voltage) are agreed, starting from the electrical state corresponding to market clearing (i.e., P^0, Q^0, V^0) to eventually converge to the optimal values ($P^{TD\star}$, $Q^{TD\star}$, $V^{TD\star}$). The lower part of the figure shows the sequence of these steps in the DSO space of PQ charts (depicted with green color), each number corresponding to the computation step at either TSO or DSO. Note that the proposed approach avoids the effort to compute the full PQ chart, computing instead only four points of it: the active power range (step 1 and its two associated points) and, for a given active power flow $P^{TD\star}$, the reactive power range (step 3 and its two associated points). Observe that the active power range fully exploits the PQ chart capability while the reactive power range could be sub-optimal as is done for a fixed $P^{TD\star}$. This is the price to pay for establishing the cost of ADS aggregated flexibility.

In a nutshell, based on this figure, the proposed five stage TSO–DSO coordination works in the following way:

1. The DSO computes the active power flexible range ($\underline{P}$, $\bar{P}$) and the associated cost (cost P).
2. If the TS is congested, the TSO procures from the global market at minimum cost AS for congestion management including active power ranges and costs provided by the DSOs. This step establishes the agreed active power flows scheduled at the TSO–DSOs interfaces ($P^{TD\star}$).
3. The DSO computes the reactive power flexible range ($\underline{Q}$, $\bar{Q}$) and the associated cost (cost Q).
4. If the TS experiences voltage issues, the TSO procures from the global market at minimum cost AS for voltage support including reactive power ranges and costs provided by the DSOs. This step establishes the agreed reactive power flows and voltages (as a by-product) at the TSO–DSOs interfaces ($Q^{TD\star}$ and $V^{TD\star}$).
5. The DSO procures and dispatches, at minimum cost from the local market, flexible resources internally so that to maintain the active and reactive power flows agreed with the TSO at steps 2 and 4 ($P^{TD\star}$ and $Q^{TD\star}$) and voltage $V^{TD\star}$ while satisfying distribution system constraints. Note that the presence of OLTC at TSO–DSO interface is an additional powerful means to easily comply with the voltage $V^{TD\star}$, the OLTC basically "decoupling" the voltage between TSO and DSO.

The complete flow chart of this 5-step approach is shown in Fig. 2. Note that the sequence of AS procurement is not strict and to be decided by the TSO, meaning that a TSO can first procure the reactive power and then the active power. In such a case, modules P and Q will replace each other in the presented flow chart. Furthermore, TSO does not need to procure both active and reactive powers if it experiences either congestion or voltage issue in the TS. In the case of congestion (no voltage issues) in a TS, only active power AS is required by the TSO. Hence under such scenario, the proposed methodology will consist only of modules P and $OPRD$. However, for the sake of describing completely the proposed methodology, this work assumes that TSO procures both active and reactive powers in the sequence shown in Fig. 2. Finally, the OP formulation of each of the five steps are presented in sections III and IV.

Before proceeding further, note that the proposed coordination scheme does not have a feedback loop per se; hence the terminology 'coordination' might mislead the readers. However, as stated above, we have assumed that energy and reserve markets are cleared before AS markets and as such, grid *unconstrained* market-desired active and reactive power flows between TSO and DSOs are known. As such, the proposed coordination scheme computes the possible deviations of active/reactive power flows, with respect to the grid-unconstrained market-desired ones at TSO–DSO interface, if network constraints are violated in either transmission or distribution system. These deviations are calculated by ensuring that all constraints are met in both transmission and distribution systems. Accordingly, the coordination scheme implies *intrinsically* the feedback loop, which has maximum two iterations (one per stage for active and reactive power, respectively) between TSO and DSOs.

Furthermore note that the proposed coordination approach does not give direct access to TSO to schedule DER, which are hosted in distribution systems. Rather, TSO and DSO only schedule the power flows (active/reactive) at their interface (substation) based on the ranges of active and reactive powers calculated by the DSO and for which the operation of the distribution system is feasible. In nutshell, both TSO and DSO have access to the DER flexibility but only through DSO.

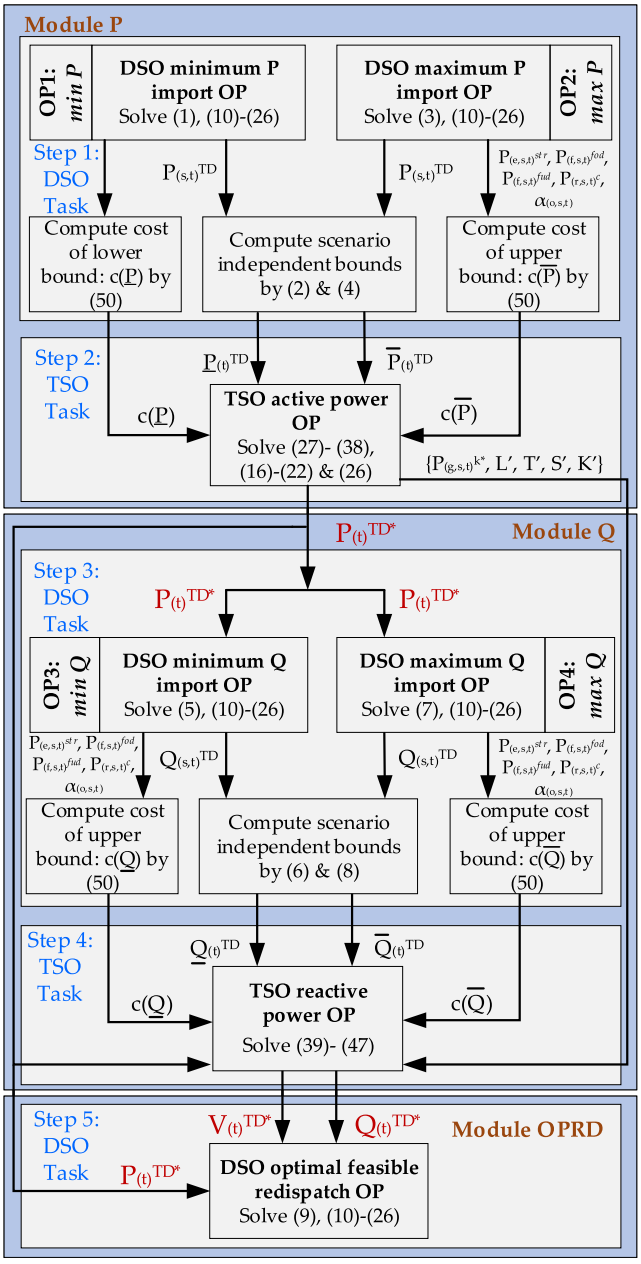

Fig. 2. Flowchart of the proposed coordination methodology.

However, under stressed operating condition, DSO has the priority to utilize DER locally in a best possible way to satisfy ADS constraints, which can reduce the available range of flexibility to TSO. To summarize, the proposed approach is a *straight forward coordination mechanism* since TSO supports and is supported by the DSO, while the DSO uses DER flexibility to meet the constraints of ADS and, if requested and has sufficient remaining flexibility on DER, also supports the TSO. Accordingly, both TSO and DSO benefit from this coordination. Finally, note that to fully release the potential flexibility from DER, there is still need to properly coordinate the access of resources and data management between TSO and DSO as reported in [23].

We opt for the proposed five-stage coordination mechanism due to its affordable overall computational burden, which fosters its possible practical implementation in real world. This is aligned with current efforts in Germany that also emphasize the importance of a small number of iterations between TSO and DSOs [26]. In comparison to the proposed coordination approach, other approaches in the literature use sophisticated decomposition techniques such as ADMM [11]) or Nash-games [21] to solve sequentially OPs at either TSO or DSO levels, which requires solving an OP at either level a significant number (possibly tens to hundreds of times [11]), provided the OP at either level converges. Accordingly, their practical implementation in the day-ahead network operation is difficult, if not impossible, to achieve.

3. Optimization problems of ADSs

The OPs of ADSs are divided into three sub-modules. The first two modules (*module P* and *module Q*) compute the range of most probable active and reactive power flexibility at TSO–DSO interface, respectively. Each module in turn handles two OPs computing the lower and upper bounds of a power range by solving minimization and maximization OPs, respectively. The third module i.e., OPRD, computes the optimal flexibility re-dispatch of distributed energy resources (DER) once optimum active and reactive set-points are set at the TSO–DSO interface through a minimization OP. Note that the proposed coordination approach is uncertainty-aware, which means the provided flexibility range of active/reactive power flows is the most probable outcome regarding flexibility potential of considered DERs.

3.1. Module P: DSO active power flexibility range

This module determines the range of active power flexibility at TSO–DSO interface by solving, possibly in parallel, two separate OPs (OP1 and OP2), which compute the lower and upper bounds of active power flexibility range, respectively.

3.1.1. OP1 (minP)

Lower P flexibility limit is defined as:

$$\min \sum_{s\in S}\sum_{t\in T} P_{s,t}^{TD} \tag{1}$$

subject to (10)–(26). After solving OP1, (2) estimates the lower bound of active power flexibility during each time period t.

$$\underline{P}_t^{TD} = \sum_{s\in S} \pi_s * P_{s,t}^{TD} \tag{2}$$

3.1.2. OP2 (maxP)

Upper P flexibility limit is defined as:

$$\max \sum_{s\in S}\sum_{t\in T} P_{s,t}^{TD} \tag{3}$$

subject to (10)–(26). After solving OP2, (4) estimates the upper bound of active power flexibility during each time period t.

$$\overline{P}_t^{TD} = \sum_{s\in S} \pi_s * P_{s,t}^{TD} \tag{4}$$

3.2. Module Q: DSO reactive power flexibility range

This module determines the range of reactive power flexibility at TSO–DSO interface by solving, possibly in parallel, two separate OPs (OP3 and OP4), which determine the lower and upper bounds of flexibility range, respectively. Furthermore, this module also maintains the committed active power flow with TSO at TSO–DSO interface, see step 3 in Fig. 2.

3.2.1. OP3 (minQ)

Lower Q flexibility limit is defined as:

$$\min \sum_{s\in S}\sum_{t\in T} \left\{ Q_{s,t}^{TD} + c_p^{viol}(P_{s,t}^{TD} - P_t^{TD^*})^2 \right\} \tag{5}$$

subject to (10)–(26). After solving OP3, (6) estimates the lower bound of reactive power flexibility during each time period t.

$$\underline{Q}_t^{TD} = \sum_{s\in S} \pi_s * Q_{s,t}^{TD} \tag{6}$$

3.2.2. OP4 (maxQ)

Upper Q flexibility limit is defined as:

$$\max \sum_{s\in S}\sum_{t\in T}\left\{Q^{TD}_{s,t} - c^{viol}_{p}(P^{TD}_{s,t} - P^{TD^*}_{t})^2\right\} \tag{7}$$

subject to (10)–(26). After solving OP4, (8) estimates the upper bound of reactive power flexibility during each time period t.

$$\overline{Q}^{TD}_{t} = \sum_{s\in S}\pi_s * Q^{TD}_{s,t} \tag{8}$$

3.3. Module OPRD: Optimal flexibility re-dispatch for DSO

This module, defined in (9), optimally re-dispatches the flexible DER, once active and reactive powers are set at TSO–DSO interface, to ensure the safe operation of ADS.

$$\begin{aligned}&\min \sum_{s\in S}\sum_{t\in T}\pi_s\{(\sum_{r\in R}c^c_r P^c_{r,s,t} + \sum_{e\in E}c_e(P^{dch}_{e,s,t} - P^{ch}_{e,s,t}) + \\ &\sum_{f\in F}c_{fl}(P^{fod}_{f,s,t} + P^{fud}_{f,s,t}) + c^{viol}_{p}(P^{TD}_{s,t} - P^{TD^*}_{t})^2 + \\ &c^{viol}_{q}(Q^{TD}_{s,t} - Q^{TD^*}_{t})^2 + c^{viol}_{v}(V^{TD}_{s,t} - V^{TD^*}_{t})^2)\Delta T \\ &+ c_{oltc}\cdot\kappa_{o,s,t}\}\end{aligned} \tag{9}$$

subject to (10)–(26). The objective (9) minimizes the expected cost of DER deviation from the market schedule in each scenario s and time period t meeting ADS constraints.

Note that in (5), (7) and (9), $P^{TD^*}_{t}$ is the procured active power (the output of Section 4.1), and $Q^{TD^*}_{t}/V^{TD^*}_{t}$ in (9) corresponds to the procured reactive power/agreed voltage at TSO–DSO interface (the output of Section 4.2).

3.4. Active distribution system constraints

The ADS OP obeys the following constraints ($\forall t \in T, s \in S$):

$$\begin{aligned}&P^{TD}_{s,t} + \sum_{r\in R}(P^0_{r,s,t} - P^c_{r,s,t}) + \sum_{e\in E}(P^{dch}_{e,s,t} + P^{ch}_{e,s,t}) - \{P^d_{n,t} \\ &+ \sum_{f\in F}(P^{fod}_{f,s,t} - P^{fud}_{f,s,t})\} = -\sum_{m\in N}\{g_{nm}(e_{n,s,t}e_{m,s,t} + f_{n,s,t} \\ &f_{m,s,t}) + b_{nm}(f_{n,s,t}e_{m,s,t} + e_{n,s,t}f_{m,s,t})\} \quad \forall n \in N\end{aligned} \tag{10}$$

$$\begin{aligned}&Q^{TD}_{s,t} + \sum_{r\in R}\tan(\phi_{r,s,t})P^0_{r,s,t} - \{\tan(\varphi_{f,s,t})\sum_{f\in F}(P^{fod}_{f,s,t} - \\ &P^{fud}_{f,s,t}) + Q^d_{n,t}\} = -\sum_{m\in N}b_{nm}(e^2_{n,s,t} + f^2_{n,s,t}) + \sum_{m\in N}\{b_{nm} \\ &(e_{n,s,t}e_{m,s,t} + f_{n,s,t}f_{m,s,t}) - g_{nm}(f_{n,s,t}e_{m,s,t} - e_{n,s,t} \\ &f_{m,s,t})\} \quad \forall n \in N\end{aligned} \tag{11}$$

$$\underline{P}^{TD} \le P^{TD}_{s,t} \le \overline{P}^{TD} \tag{12}$$

$$\underline{Q}^{TD} \le Q^{TD}_{s,t} \le \overline{Q}^{TD} \tag{13}$$

$$0 \le P^c_{r,s,t} \le P^0_{r,s,t} \quad \forall r \in R \tag{14}$$

$$-\tan(\overline{\phi}_{r,s,t}) \le \tan(\phi_{r,s,t}) \le \tan(\overline{\phi}_{r,s,t}) \quad \forall r \in R \tag{15}$$

$$0 \le P^{fod}_{f,s,t}/P^{fud}_{f,s,t} \le D\cdot P^{fd}_{f,s,t} \quad \forall f \in F \tag{16}$$

$$\sum_{t\in T}P^{fod}_{f,s,t}\cdot\Delta T = \sum_{t\in T}P^{fud}_{f,s,t}\cdot\Delta T \quad \forall f \in F \tag{17}$$

$$-P^{ch,rat}_{e} \le P^{ch}_{e,s,t} \le 0 \quad \forall e \in E \tag{18}$$

$$0 \le P^{dch}_{e,s,t} \le P^{dch,rat}_{e} \quad \forall e \in E \tag{19}$$

$$SoC_{e,s,t} - SoC_{e,s,t-1} = \frac{\Delta T}{E^r_e}(-\eta^{ch}_e P^{ch}_{e,s,t} - \frac{P^{dch}_{e,s,t}}{\eta^{dch}_e}) \tag{20}$$

$$\underline{SoC}_e \le SoC_{e,s,t} \le \overline{SoC}_e \quad \forall e \in E \tag{21}$$

$$SoC_{e,s,t_n} = SoC_{e,s,t_0} \quad \forall e \in E \tag{22}$$

$$\underline{V}^2_n \le (e^2_{n,s,t} + f^2_{n,s,t}) \le \overline{V}^2_n \quad \forall n \in N \tag{23}$$

$$\underline{\alpha}_o \le \alpha_{o,s,t} \le \overline{\alpha}_o \quad \forall o \in O \tag{24}$$

$$|\alpha_{o,s,t} - \alpha^0_{o,s,t}| \le \kappa_{o,s,t} \quad \forall o \in O \tag{25}$$

$$\begin{aligned}&(g^2_{nm} + b^2_{nm})\{(e_{n,s,t} - e_{m,s,t})^2 + (f_{n,s,t} - f_{m,s,t})^2\} \le \\ &\overline{I}^2_{l,s,t} \quad \forall l \in L\end{aligned} \tag{26}$$

where (10) and (11) are the active and reactive power balance constraints, (12) and (13) are the limits on active and reactive power flows at TSO–DSO interface, (14) models the active power curtailment of RES units, (15) represents the adaptive power factor constraint on RES units, (16) is the limit on over/under demand of active power of FLs, (17) maintains the energy balance of FLs over whole horizon, (18) and (19) are limits on active power charging and discharging of EES, (20) models the EES energy balance, (21) constraints the state-of-charge (SoC), (22) maintains the SoC of EES equal on the first and last time periods, (23) is the limit on each bus voltage magnitude, (24) models the tap-ratio constraint (not explicitly shown in (10) and (11) to lighten the formulation), (25) models the absolute of deviation of transformer ratio from its initial value in the objective function (i.e., $|\alpha_{o,s,t} - \alpha^0_{o,s,t}|$) and (26) represents the branch current limits. Finally, the presence of EES' charging and discharging terms in objective (9) prohibits anytime its simultaneous charging and discharging [27].

4. Optimization problems of transmission system

The OPs of TS consist of two modules, see steps 2 and 4 in Fig. 2. The *module P* finds the optimal active power re-dispatch of conventional generators and optimal active power flow at TSO–DSO interface for congestion management. Likewise, the *module Q* determines the optimal reactive power set points of conventional generators and optimal reactive power flow at TSO–DSO interface for voltage control purposes.

4.1. Module P: TSO active power optimization problem

The TSO active power OP minimizes the expected cost of AS procurement (congestion management), cost of deviation of conventional generators, EESs and FLs from market schedule, and cost of RES and load curtailment in each scenario s and time period t under both normal and post contingencies states as shown in (27).

$$\begin{aligned}&\min \sum_{s\in S}\sum_{t\in T}\pi_s\{\sum_{g\in G}c_g\left(P^0_{g,s,t} - P^{\star}_{g,t}\right) \\ &+ \sum_{k\in K}(\sum_{e\in E}c_e(P^{dch,k}_{e,s,t} - P^{ch,k}_{e,s,t}) + \sum_{f\in F}c_{fl}(P^{fod,k}_{f,s,t} + P^{fud,k}_{f,s,t}) \\ &+ \sum_{r\in R}c^c_r P^{c,k}_{r,s,t} + \sum_{n\in N}c^c_n(P^{c,k}_{n,s,t}) + \sum_{n\in N}Z^{p,flx}_{n,s,t})\}\end{aligned} \tag{27}$$

The problem is subjected to (16)–(22) & (26) and the following constraints ($\forall t \in T, s \in S, k \in K$):

$$\begin{aligned}&P^{TD}_{n,s,t} + \sum_{g\in G}P^k_{g,s,t} + \sum_{r\in R}(P^0_{r,s,t} - P^{c,k}_{r,s,t}) + \sum_{e\in E}(P^{dch,k}_{e,s,t} \\ &- P^{ch,k}_{e,s,t}) - \{(P^d_{n,t} - P^{c,k}_{n,s,t}) + \sum_{f\in F}(P^{fod,k}_{f,s,t} - P^{fud,k}_{f,s,t})\} \\ &= -\sum_{m\in N}\{g_{nm}(e^k_{n,s,t}e^k_{m,s,t} + f^k_{n,s,t}f^k_{m,s,t}) + \\ &b_{nm}(f^k_{n,s,t}e^k_{m,s,t} - e^k_{n,s,t}f^k_{m,s,t})\} \quad \forall n \in N\end{aligned} \tag{28}$$

$$\begin{aligned}&\sum_{g\in G}Q^k_{g,s,t} - (Q^d_{n,t} - Q^{c,k}_{n,s,t}) = -\sum_{m\in N}b_{nm}(e^{k^2}_{n,s,t} + \\ &f^{k^2}_{n,s,t}) + \sum_{m\in N}\{b_{nm}\left(e^k_{n,s,t}e^k_{m,s,t} + f^k_{n,s,t}f^k_{m,s,t}\right) \\ &- g_{nm}\left(f^k_{n,s,t}e^k_{m,s,t} - e^k_{n,s,t}f^k_{m,s,t}\right)\} \quad \forall n \in N\end{aligned} \tag{29}$$

$$\underline{P}_g(\underline{Q}_g) \le P^k_{g,s,t}(Q^k_{g,s,t}) \le \overline{P}_g(\overline{Q}_g) \quad \forall g \in G \tag{30}$$

$$\underline{P}_t^{TD} \le P_{n,s,t}^{TD} \le \overline{P}_t^{TD} \qquad \forall n \in N \tag{31}$$

$$\left|P_{g,s,t-1}^{0} - P_{g,s,t}^{0}\right| \le \Delta P_g \qquad \forall g \in G \tag{32}$$

$$\left|P_{g,s,t}^{k} - P_{g,s,t}^{0}\right| \le \Delta P_g \qquad \forall g \in G, k \ne 0 \tag{33}$$

$$0 \le P_{n,s,t}^{c,k} \le P_{n,s,t}^{d}, \qquad \forall n \in N \tag{34}$$

$$0 \le P_{r,s,t}^{c,k} \le P_{r,s,t}^{0}, \qquad \forall n \in N \tag{35}$$

$$\underline{V}_n^2 \le (e_{n,s,t}^{k^2} + f_{n,s,t}^{k^2}) \le \overline{V}_n^2 \qquad \forall n \in N(G) \tag{36}$$

$$slp_{n,s,t}^{p,flx,1} P_{n,s,t}^{TD} + d_{n,s,t}^{p,flx,1} \le Z_{n,s,t}^{p,flx} \tag{37}$$

$$slp_{n,s,t}^{p,flx,2} P_{n,s,t}^{TD} + d_{n,s,t}^{p,flx,2} \le Z_{n,s,t}^{p,flx} \tag{38}$$

where (28) and (29) represent the active and reactive power balance constraints, (30) is the hard physical limits on active (reactive) power of a generator, (31) restricts the active power flexibility, needed to be procured, by the TSO at TSO–DSO interface between the lower and upper bounds, which are provided by the DSOs OP1 and OP2, (32) restricts the ramping of a generator in two successive time intervals under normal operation, (33) couples the active power of a generator between normal operation and post-contingency states, (34) limits the load curtailment, (35) restricts the RES curtailment, (36) is the limit on each bus voltage magnitude, and (37) and (38) represent the V-shaped linear approximated cost function of active power flexibility through an auxiliary variable $Z_{n,s,t}^{p,flx}$ (see Section 5 for details on $slp_{n,s,t}^{p,flx,1/2}$ and $d_{n,s,t}^{p,flx}$).

4.2. Module Q: TSO reactive power optimization problem

The reactive power OP minimizes the expected cost of AS procurement (voltage control) in TS operation under both normal and post contingency states as shown in (39).

$$\min \sum_{s\in S}\sum_{t\in T}\{\sum_{k\in K}\pi_s \sum_{g\in G}|Q_{g,s,t}^{k}| + \sum_{n\in N} Z_{n,s,t}^{q,flx}\} \tag{39}$$

The problem is subject to the following constraints ($\forall t \in T, s \in S, k \in K$):

$$\begin{aligned}
&P_{n,s,t}^{TD^*} + \sum_{g\in G/slack} P_{g,s,t}^{k^*} + P_{slack,s,t}^{k} + \sum_{e\in E}(P_{e,s,t}^{dch,k^*} - \\
&P_{e,s,t}^{ch,k^*}) + \sum_{r\in R}(P_{r,s,t}^{0} - P_{r,s,t}^{c,k^*}) - \{(P_{n,t}^{d} - P_{n,s,t}^{c,k^*}) + \sum_{f\in F} \\
&(P_{f,s,t}^{fod,k^*} - P_{f,s,t}^{fud,k^*})\} = -\sum_{m\in N}\{g_{nm}(e_{n,s,t}^{k} e_{m,s,t}^{k} + f_{n,s,t}^{k} \\
&f_{m,s,t}^{k}) + b_{nm}(f_{n,s,t}^{k} e_{m,s,t}^{k} - e_{n,s,t}^{k} f_{m,s,t}^{k})\} \quad \forall n \in N
\end{aligned} \tag{40}$$

$$\begin{aligned}
&\sum_{g\in G} Q_{g,s,t}^{k} + Q_{n,s,t}^{TD} - (Q_{n,t}^{d} - Q_{n,s,t}^{c,k}) = -\sum_{m\in N}(b_{nm}) \\
&(e_{n,s,t}^{k^2} + f_{n,s,t}^{k^2}) + \sum_{m\in N}\{b_{nm}\left(e_{n,s,t}^{k} e_{m,s,t}^{k} + f_{n,s,t}^{k} f_{m,s,t}^{k}\right) \\
&- g_{nm}\left(f_{n,s,t}^{k} e_{m,s,t}^{k} - e_{n,s,t}^{k} f_{m,s,t}^{k}\right)\} \qquad \forall n \in N
\end{aligned} \tag{41}$$

$$\underline{Q}_t^{TD} \le Q_{n,s,t}^{TD} \le \overline{Q}_t^{TD} \qquad \forall n \in N \tag{42}$$

$$\underline{Q}_g \le Q_{g,s,t}^{k} \le \overline{Q}_g \qquad \forall g \in G \tag{43}$$

$$\underline{V}_n^2 \le (e_{n,s,t}^{k^2} + f_{n,s,t}^{k^2}) \le \overline{V}_n^2 \qquad \forall n \in N \tag{44}$$

$$\begin{aligned}
&(g_{nm}^2 + b_{nm}^2)\left[\left(e_{n,s,t}^{k} - e_{m,s,t}^{k}\right)^2 + \left(f_{n,s,t}^{k} - f_{m,s,t}^{k}\right)^2\right] \\
&\le \overline{I}_{l,s,t}^2 \qquad \forall l \in L', s \in S', t \in T', k \in K'
\end{aligned} \tag{45}$$

$$slp_{n,s,t}^{q,flx,1} Q_{n,s,t}^{TD} + d_{n,s,t}^{q,flx,1} \le Z_{n,s,t}^{q,flx} \tag{46}$$

$$slp_{n,s,t}^{q,flx,2} Q_{n,s,t}^{TD} + d_{n,s,t}^{q,flx,2} \le Z_{n,s,t}^{q,flx} \tag{47}$$

where (40) is the active power balance constraint set by fixing the active power (TSO *module P* results) at: TSO–DSO interface, conventional generators in all states (except slack generator), charging state of EESs, FLs, generation and load shedding under the same scenario (fixed values are marked by *), (41) is the reactive power balance for all operation states, (42) restricts the reactive power flexibility, needed to be procured, by the TSO at TSO–DSO interface between the lower and upper bounds provided by the DSOs OP3 and OP4, (43) limits the reactive power of generators, (44) limits the voltages at all nodes, (45) represents the branch current limit for a limited subset of congested cases (TSO *module P* results), and (46) and (47) are the V-shaped linear approximated cost function of reactive power flexibility being procured by the TSO (see Section 5 for details on $slp_{n,s,t}^{q,flx,1/2}$ and $d_{n,s,t}^{q,flx}$).

5. Cost of active and reactive power flexibility

Apart from the range of flexibility that DSOs can make available at TSO–DSO interface, they also need to provide the cost of this flexibility to allow TSO to procure the optimal amount of flexibility from ADSs.

To approximate the cost of active and reactive power flexibility, we assume that the initial active power set-points of DER and associated initial cost to these set-points are known after energy market clearing. Based on this, the cost of lower and upper bounds of active (48) and reactive (49) power flexibility, determined in OP1-OP4, are computed as:

$$\begin{aligned}
c_{s,t}^{P,flx} = &\sum_{e\in E} c_e |P_{e,s,t}^{str^\star} - P_{e,s,t}^{str}| + \sum_{a\in A}|\alpha_{o,s,t}^{\star} - \alpha_{o,s,t}| \\
&+ \sum_{f\in F} c_{fl}|P_{f,t}^{d^\star} - (P_{f,t}^{d} + (P_{f,s,t}^{od} - P_{f,s,t}^{ud}))| \\
&+ \sum_{r\in R} c_r^c |P_{r,s,t}^{0^\star} - (P_{r,s,t}^{0} - P_{r,s,t}^{c})|
\end{aligned} \tag{48}$$

$$c_{s,t}^{Q,flx} = c_{s,t}^{P,flx} + c_p^{viol}|P_t^{TD^*} - \sum_{s\in S}\pi_s \cdot P_{s,t}^{TD}| \tag{49}$$

where * in the superscript indicates the values of relative terms $(P_{e,s,t}^{str^\star}, P_{f,s,t}^{fd^\star}, P_{r,s,t}^{0^\star}, \alpha_{o,s,t}^{\star})$ obtained after energy market clearing. Based on (48) and (49), two costs $\{c_{s,t}^{P/Q,flx}(\underline{P},\underline{Q}),\ c_{s,t}^{P/Q,flx}(\overline{P},\overline{Q})\}$ per time period and scenario are available; they correspond to the lower and upper active/reactive power bounds, after solving *module P* and *module Q* ADS OPS, see Fig. 2. Finally, (50) provides the resultant weighted costs per time period which are embedded in the global AS market.

$$c_t^{x,flx} = \sum_{s\in S}\pi_s \times c_{s,t}^{x,flx} \tag{50}$$

where $x \in (P, Q)$. The two calculated costs lead to a V-shaped cost function (see Fig. 1), where the middle point represents the operation cost of DER after energy market clearing, and two extreme points represent the calculated cost terms of lower and upper bounds of active and reactive power range. *Note that, the V-shape cost function is used to avoid the computation burden of a more accurate (piece-wise) linear approximation, where the desired number of problems for active and reactive power should be solved by the DSO. Nevertheless, an approximation of improved accuracy can be easily utilized at the expense of computation time increase.*

After availability of cost values (50) of active/reactive power flexibility, TSO can embed $c_t^{x,flx}$ in its OPs to determine the cost optimum flexibility that it can procure as shown below.

$$slp_{n,s,t}^{x,flx,1} = \frac{c_{n,t}^{x,flx}(\underline{x}) - 0}{\underline{x}_{n,t}^{TD} - x_{n,t}^{TD,\star}}; \quad d_{n,s,t}^{x,flx,1} = slp_{n,s,t}^{x,flx,1} x_{n,t}^{TD,\star} \tag{51}$$

$$slp_{n,s,t}^{x,flx,2} = \frac{c_{n,t}^{x,flx}(\overline{x}) - 0}{\overline{x}_{n,t}^{TD} - x_{n,t}^{TD,\star}}; \quad d_{n,s,t}^{x,flx,2} = slp_{n,s,t}^{x,flx,2} x_{n,t}^{TD,\star} \tag{52}$$

In (51) and (52), $slp^{1/2}$ and $d^{1/2}$ are the first/second coefficient multipliers and constant coefficients to determine the slope of linear cost function associated with x, $x \in (P, Q)$, $\underline{x}$ and $\bar{x}$ represent the lower and upper bounds of flexibility (the output of *modules P* and *Q* ADS OPs, which are indexed by n in TSO OPs for each flexibility node) and $X^\star$ represents the initial flow at TSO–DSO interface after energy market clearing (any deviation from this point will impose an additional cost).

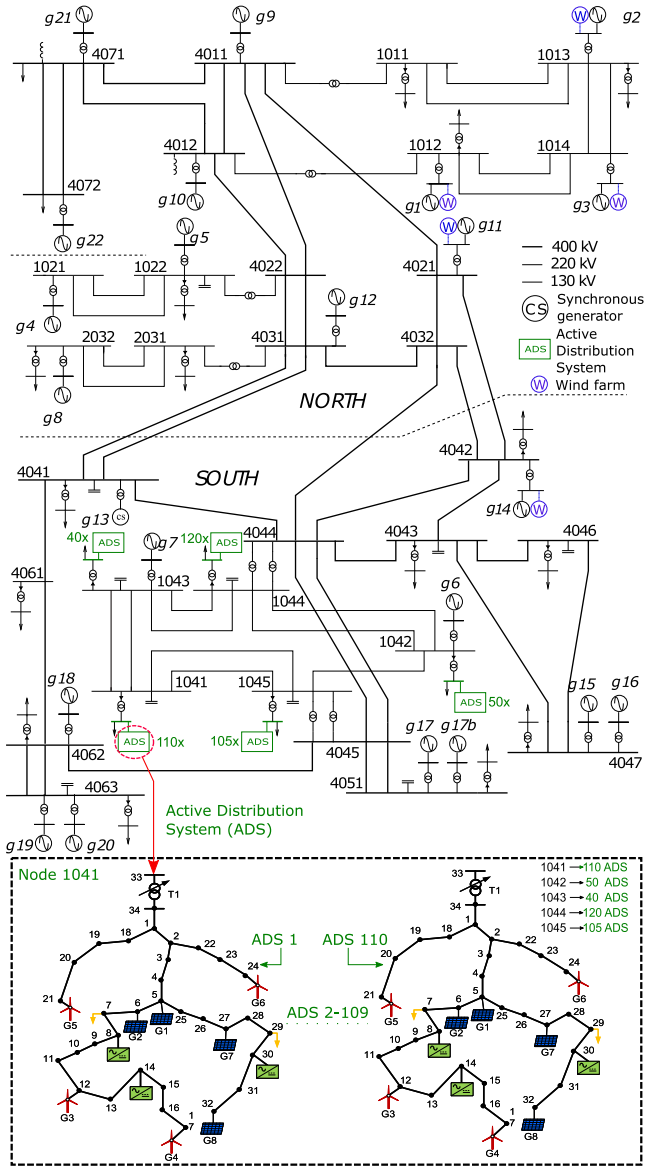

Fig. 3. Nordic32 60-bus TS connected to five 34-bus ADSs.

6. Case study

6.1. General assumptions for the TS and the ADSs

The proposed methodology is tested on a power system consisting of a 60-bus Nordic32 TS [28], to which five ***flexibility providing*** ADSs are connected at nodes 1041, 1042, 1043, 1044 and 1045, as shown in Fig. 3. These nodes are termed as *flexibility nodes*. Furthermore, to each flexibility node specific number (e.g., 110 at node 1041) of 34-bus ADS [29,30] are connected in parallel to scale down the total load, as seen by the TSO, to a level which does not stress an individual 34-bus ADS. Finally, ADSs connected at different flexibility nodes have distinct load profiles, based on the load profiles at each flexibility node, from one another.

The proposed approach considers, for both TS and ADSs, 24 time periods (hourly resolution) and 10 uncertainty scenarios for solar and wind RES which are generated by an ARIMA model [31]. Both NLP S-MP-SCOPF (TS) and S-MP-OPF (ADS) OPs are developed in Julia/JuMP [32] and are solved using IPOPT [33], executed with default settings.

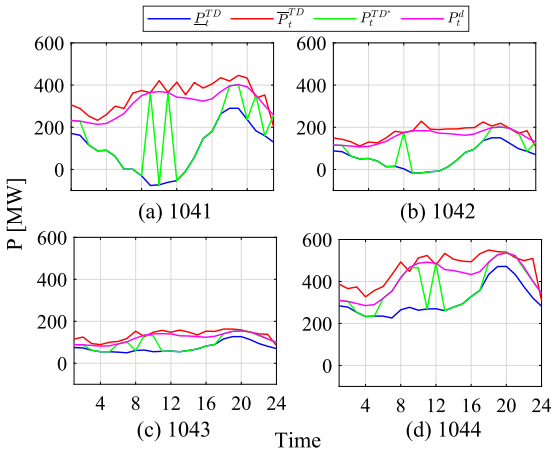

Fig. 4. Lower and upper active power bounds from DSO and procured flexibility by TSO at TSO–DSO interface.

Lastly, in the TS, a set of 33 N-1 line contingencies is assumed. Moreover, five wind farms with capacity 7.2, 5.4, 6.3, 5.7 and 6.3 GW are considered. In the ADS, eight RES (1 MW) and three ESSs (1 MWh) capacity are considered along with two FLs with up to 50% flexible demand.

6.2. Results of proposed AS procurement methodology

This section presents the results of different stages (steps 1 to 5) of the proposed AS procurement methodology.

6.2.1. Provision of active power flexibility range by DSO and procurement of flexibility by TSO

Fig. 4 shows the results of *module P* of AS procurement algorithm. Following observations can be made from the presented results.

Under a large active power production by renewable RES, DSOs at each flexibility node can provide a substantial amount of flexibility as compared to the active power flow at TSO–DSO interface in the absence of any DER in the ADS. For example, the maximum available flexibility that can be provided at each node varies between 85 MW (1043) and 450 MW (1041) for OP1 (i.e., lower limit) and between 30 MW (1043) and 110 MW (1044) for OP2 (i.e., upper limit). These values indicate that ADSs can play a very effective role in managing congestion in their upstream TS by increasing/decreasing the active power flow at TSO–DSO interface.

It can also be observed that the width of flexibility band varies at each flexibility node which indicates that different DSOs provide distinct flexibility range at their point of interconnection; thus imitating a real-world scenario. Moreover, the shape of flexibility band largely depends upon the power production profiles of RES. During time-periods 8 h–16 h, the range becomes wider at all flexibility nodes as compared to the range during time periods 1 h–8 h and 17 h–24 h. This is mainly due to the large active power production during time-periods 8 h–16 h from solar RES, which leads to more local utilization and curtailment when OP1 and OP2 are solved, respectively. This contrasts with the time periods 1 h–8 h and 17 h–24 h where large share of active power predominantly flows from the TSO towards DSO (due to no solar and less wind generation). Moreover, DSOs at nodes 1041 and 1042 can inject/absorb active power to/from the TS, whereas DSOs at nodes 1043 and 1044 can only absorb active power from the TS. Nevertheless, the latter DSOs can still provide flexibility by either increasing or decreasing the total load as seen from the TSO.

To verify the impact of procured flexibility in relieving congestion in the studied TS, it can also be noticed from Fig. 4 that: (i) during large time-periods over the complete horizon, TSO procures flexibility

Table 2
Cost (€) of activation of ADSs flexibility by TSO.

	Without activated Flex.	Activated Flex.
Operation	151,145	141,437
Normal Gen. curt.	18,425	18,375
Post-contin. Gen. curt.	29,784	29,753
Flexibility	–	3268
Total cost	199,354	192,833
Elapsed time (s)	2445	2449

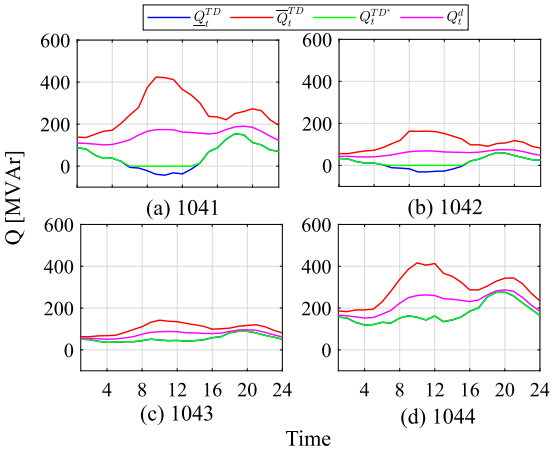

Fig. 5. Lower and upper reactive power bounds from DSO and procured flexibility by TSO at TSO–DSO interface.

equal to the lower bound of active power range (i.e., active power flow at TSO–DSO interface is *lowered* as compared to the initial case after energy market clearing), (ii) the procured flexibility does not exceed the total load seen in the downstream ADSs as it can increase the chances of congestion in the TS, (iii) the procured flexibility differs at each flexibility node and (iv) the procurement of flexibility reduces the total operation cost of the TS. The latter is further corroborated by the operation cost values, shown in Table 2, with and without procurement of active power flexibility from ADSs. It can be observed that the major cost reduction of 9708€ occurs in normal operation, whereas the overall cost reduction becomes 6521€ when the flexibility is procured by the TS. This advocates that the procurement of active power flexibility from ADSs can lead to a more cost-optimal operation of TS as compared to business as usual (i.e., without DSOs' flexibility).

6.2.2. Provision of reactive power flexibility range by DSO and procurement of flexibility by TSO

Fig. 5 shows the results of *module Q* of AS procurement algorithm. Following observations can be made from the presented results.

Like *module P*, it can be noticed that DSOs can lower down the reactive power import in the range of 44 MVAr (1043)–211 MVAr (1041) during OP3, while DSOs can increase the import of reactive power in the range of 55 MVAR (1043)–252 MVAr (1041) during OP4. Furthermore, unlike lower and upper active power bounds in Fig. 4, the minimum and maximum reactive power bounds in Fig. 5 are more uniformly distributed around the *initial* reactive power demand (seen by TSO after energy market clearing). This indicates that DSOs can offer the TSO more "freedom" during both over-voltage and under-voltage scenarios.

Furthermore, during *module Q* OP, the agreed active power at TSO–DSO interface must be respected as long as the OP of DSO remains feasible. However, under stressed operating condition, DSO is not obliged to fulfill accurately its commitment and can move away from the agreed active power flow to maintain the safe operation of its system. In this regard, Fig. 6 compares the committed active power

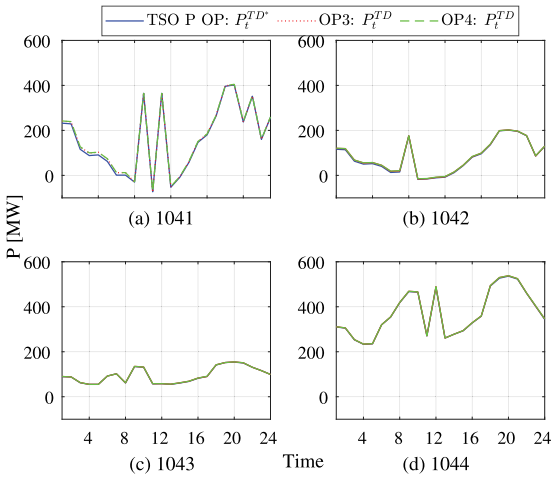

Fig. 6. Active power flow at TSO–DSO interface in OP3 and OP4, and its comparison with the agreed active power determined in module P TSO OP.

flow (i.e., the output of TSO active power OP) with the obtained active power flow during *module Q* ADS OPs at TSO–DSO interface. It can be seen that at nodes 1041 and 1042, the active power flow slightly deviates during time-periods 1 h–8 h, whereas in the remaining time-periods as well as for nodes 1043 and 1044, the active power flow at TSO–DSO interface is maintained at the committed value.

With respect to the procured flexibility by TSO, the reactive power export to the downstream DSOs becomes equal to the lower reactive power flexibility bound at nodes 1043 and 1044. On the other hand, the export value follows the lower flexibility curve but does not import reactive power from the downstream DSOs during time-periods 6 h–14 h at nodes 1041 and 1042. This is due to the fact that the reactive power flexibility cost is larger than the cost of reactive power from conventional generators, which puts the export/import of reactive power to/from DSOs in a lower priority than procuring the reactive power from conventional generators.

We observed that as compared to business as usual (i.e., the absence of flexibility from DSOs), the reactive power availability from conventional generators is not sufficient to ensure the feasible operation of the TS. Consequently, the TSO reactive power OP becomes infeasible as voltage limits cannot be met for some contingencies. However, by considering reactive power flexibility from DSOs, the TSO reactive power OP becomes feasible again, which proves the value of flexibility.

6.2.3. Optimal re-dispatch of active and reactive power by DSO

Fig. 7 shows the active and reactive power flows at the interface when optimal re-dispatch (OPRD) OP (step 5 of proposed approach) is solved by DSOs under binding and non-binding agreement of maintaining the active and reactive power flows at their interface with the TSO.

Firstly, it can be noticed that the deviation in active power with respect to the set-values is almost negligible at all flexibility nodes, whereas reactive power deviates to some extent, but still not significantly, from its committed value. This fact is further supported by the low operation cost, presented in Table 3, which lies within (100€–300€) per ADS (since the cost of violation is 100€/MWh (MVAr), a significant deviation from the committed value would lead to a large operation cost, which is not the case in the presented results). Secondly, it can also be noticed in Table 3 that if there is no agreed active and reactive power flow at TSO–DSO interface, there is (almost) no operation cost associated with the OPRD OP due to non-curtailment of RES generation. This allows DSO to send active power to TSO (without performing generation curtailment) in a large quantity; provided physical active and reactive power flow limits are observed at the interface.

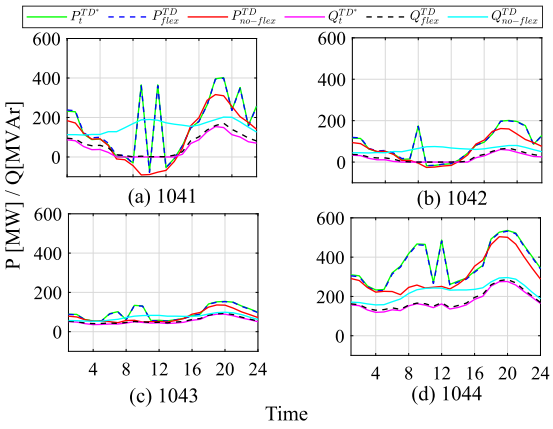

Fig. 7. Active and reactive power flows with and without flexibility provision from DSO at TSO–DSO interface.

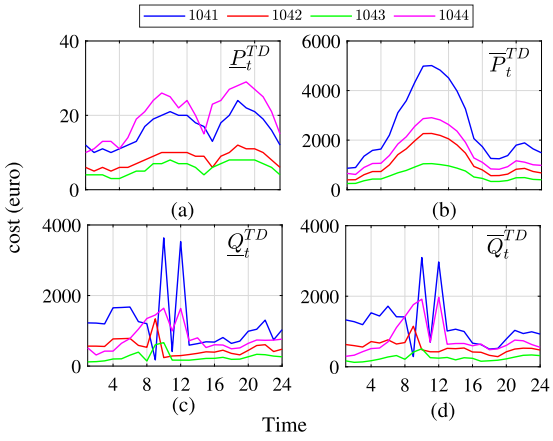

Fig. 8. Flexibility provision cost associated with the active and reactive power range: (a) OP1 (b) OP2 (c) OP3 (d) OP4.

Table 3
Optimal DSO re-dispatch module results.

Flexibility nodes	With TSO–DSO flexibility			Without TSO–DSO flexibility		
	Cost (€)	P_{curt} (MW)	Time (s)	Cost (€)	P_{curt} (MW)	Time (s)
1041	271.7	12.4	386.7	0.00037	1.11×10^{-5}	27.4
1042	235.4	9.77	470.6	0.00037	1.11×10^{-5}	27.2
1043	157.3	10.14	198.9	0.00037	1.11×10^{-5}	27.7
1044	138.5	10.63	837	0.06217	1.11×10^{-5}	26.7

6.2.4. Cost of provided active and reactive power flexibility

Fig. 8 shows the cost values associated with the obtained active and reactive power flexibility range. Firstly, it can be noticed in Fig. 8(a) and (b) that the lower and upper bounds of active power flexibility range have very low and high costs, respectively. This is mainly that almost no active power is curtailed in OP1, whereas full RES active power is curtailed in OP2. Consequently, the value of $c_r^c * |P_{r,s,t}^{0\star} - (P_{r,s,t}^{0} - P_{r,s,t}^{c})|$ term goes to zero in (48) in OP1, whereas the value of this term becomes equal to $c_r^c * P_{r,s,t}^{0\star}$ in OP2. Resultantly, a large cost value is associated to the active power bound of OP2.

On the other hand, both lower and upper reactive power flexibility bounds have almost identical cost values as shown in Fig. 8(c) and (d), respectively. As the cost of reactive power flexibility procurement is the combination of costs of re-dispatch of DER and violation of committed active power flow, two distinct observations can be made: (i) Flexibility bounds at nodes 1041 and 1042 have higher associated costs than the flexibility range at nodes 1043 and 1044 during time-periods 1 h–6 h. This stems from the fact that the agreed active power point is not strictly observed at the former nodes during these time-periods (see Fig. 6). Consequently, the violation cost term part determines the overall cost of available flexibility; (ii) During time-periods 8 h–14 h, the reactive power flexibility cost at all nodes shows a sudden increase in the form of a peak due to a large curtailment of active power from RES. Accordingly, DER re-dispatch cost term becomes dominant and dictates the overall cost of available flexibility during these time-periods.

Table 4
Computational details of DSO and TSO OPs.

Flexibility nodes	Comp. Parm.	DSO OP				TSO OP	
		minP	*maxP*	*minQ*	*maxQ*	P	Q
1041	Time (s)	111	603	93	252	Time (s)	
	Iter.	141	721	130	270		
1042	Time (s)	44	551	199	237		
	Iter.	61	795	266	298		
1043	Time (s)	30	444	57	111	2449	1480
	Iter.	45	612	79	258		
1044	Time (s)	28	421	35	80		
	Iter.	43	476	56	208		

Comp. Parm. → Computational Parameters; Iter. → Iterations.

6.2.5. Impact of different flexibility options on active power range by DSO

Fig. 9 shows the impact of various flexible options (FOs) on the active power range at node 1041. The different FOs considered are: C1 (active power curtailment-APC), C2 (APC + OLTC ratio), C3 (APC + adaptive power factor (ADPF)), C4 (APC + OLTC + ADPF), C5 (APC + ESS), C6 (APC + FLs), C7 (APC + ESS + FLs), C8 (APC + OLTC + ESS + FL). The lower active power bound in Fig. 9(a) shows that under C2 and C4 FOs, more active power can be exported from DSOs to TSO in comparison to the C1 FO. This also suggests that less active power will be curtailed by involving more FOs in the flexibility provision framework. Similarly, the upper active power bounds in Fig. 9(a) shows that under C1, less active power can be exported from TSO to DSO in comparison to the C3 and C4 FOs.

On the other hand, the upper active power bounds in Fig. 9(a) and (b) show a sharp difference when FOs involving third generation DER (ESS, FL) are used as compared to the first generation DER (APC, ADPF, OLTC ratio). The involvement of former DER in flexibility provision leads to a sharp increase/decrease in the active power import from TSO; giving larger room to TSO to manage congestion in the TS.

6.2.6. On the V-shape cost function precision

Fig. 10 shows the approximated linear cost function with the proposed 3 points and the more accurate one with 10 points for the interface bus 1041. The approximation of active power cost is reasonably accurate while the one of reactive power cost is less accurate. The precision of this linear approximation increases as new points are computed but this comes at an increase, roughly more than three times as compared to the time reported in Table 4, in the computation time for DSO in both stages 1 and 3. Accordingly, the number of points should be decided heuristically as a trade-off between the accuracy and computation time, to be agreed by TSO and DSO depending on the time constraints of the overall coordination mechanism. One can also observe that the cost of reactive power flexibility is relatively low on a wide range, which is due to the fact that the cost of DER adjustments are negligible, higher costs being the result of constraints difficult to satisfy in ADS or implicit large variation of active power losses.

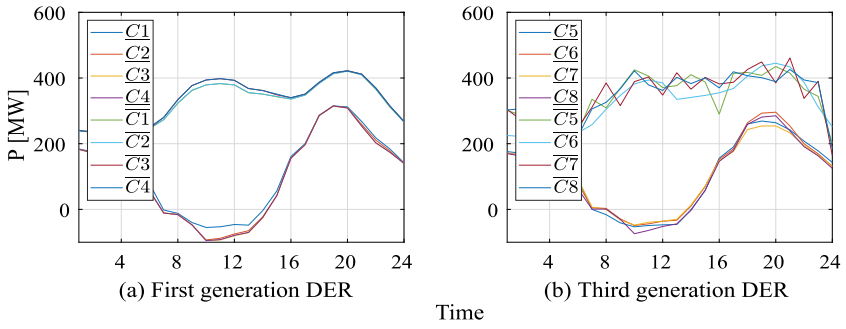

Fig. 9. Impact of several flexibility option on the active power range at flexibility node 1041.

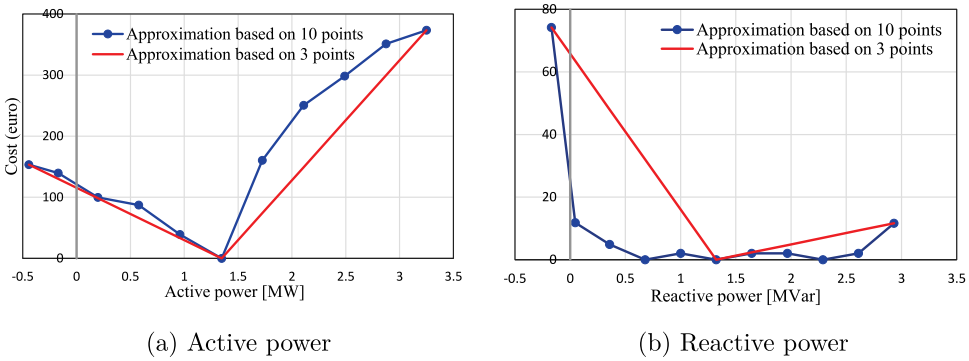

Fig. 10. Comparison between V-shape (3-points) and 10-points approximation of cost function for the interface bus 1041.

6.3. Computational performance

The computational details (solution time and solver iterations) are shown in Table 4 for both DSO and TSO OPs.

For DSO OPs, the minimization OPs (OP1 and OP3) take comparatively less time than the maximization OPs (OP2 and OP4) for all flexibility nodes. More specifically, the $minP$ and $minQ$ can be solved very fast i.e., in the time frame of 1–3 min. On the other hand, the $maxP$ and $maxQ$ OPs take approximately 7–10 and 2–5 min, respectively and are slightly computationally less efficient.

For TSO OPs, the computational time of active and reactive OPs is in the range of 30–45 min. From day-ahead operation framework point of view, the solution time for both TS and ADSs is moderate. To achieve scalability for larger real-world power systems, tractable solutions can be implemented for both systems OPs and are envisioned in future work.

7. Conclusions

This paper proposes a novel TSO–DSO coordination mechanism which enables the procurement of AS (congestion management and voltage control) by TSO from its downstream DSOs in day-ahead operation. The proposed methodology allows DSOs to provide successively the range and cost of flexible active and reactive power at TSO–DSO interface, to be embedded subsequently in the AS markets for congestion and voltage management at TSO level. Furthermore, the proposed coordination mechanism contains advanced challenging features with respect to the state-of-the-art (e.g., N-1 security in TSO OP and operation uncertainties at both TSO and DSO levels, see Table 1), which prevents a direct comparison of the proposed approach with the existing methodologies.

The presented results show that DSOs can provide a substantial amount of both active and reactive power flexibility at their point of interconnection with TSO. The available flexibility can become as large as 450 MW and 211 MVAr in the downward direction (reducing the power import from TSO to DSO) and can become as large as 110 MW and 252 MVAr in the upward direction (increasing the power flows from TSO to DSO). However, flexibility band varies in time from one node to another according to the operating conditions.

The numerical results also show that TSO procures mostly flexibility from ADSs in downward direction, often equal to the lower bounds of active and reactive power range during several time-periods. Utilizing this flexibility is valuable for the TSO as compared to the business as usual case (i.e. without flexibility from DSO) because it relieves congestion and maintains node voltages within the prescribed limits at lower TS operation cost, but especially it enables the TSO to ensure the secure operation of TS, which is impossible without DSO flexibility, as shown for the TSO reactive power OP.

Given day-ahead requirements, the overall computation effort of the proposed methodology is moderate. However, future work is planned to develop a tractable version of the proposed methodology to ensure its scalability for large size real-world power systems. This will be achieved by leveraging and adapting recently published tractable approaches for SCOPF and OPF at both TSO and DSO levels to the five optimization problems of the proposed TSO–DSO coordination. Specifically, the two SCOPF like OPs at TSO level and three OPF like OPs at DSO level can be made affordable if tractable tools are used at TSO [34] and DSO [35] levels.

CRediT authorship contribution statement

Muhammad Usman: Conceptualization, Methodology, Software, Writing – original draft, Writing – review & editing, Investigation, Validation. **Mohammad Iman Alizadeh:** Conceptualization, Methodology, Software, Writing – original draft, Writing – review & editing, Investigation, Validation. **Florin Capitanescu:** Conceptualization, Methodology, Writing – original draft, Writing – review & editing, Investigation, Validation, Supervision, Funding acquisition, Project administration.

Iason-Iraklis Avramidis: Writing – original draft, Writing – review & editing, Validation. **André Guimaraes Madureira:** Writing – original draft, Writing – review & editing, Validation, Funding acquisition.

Declaration of competing interest

The authors declare that they have no known competing financial interests or personal relationships that could have appeared to influence the work reported in this paper.

Data availability

Data will be made available on request.

Acknowledgments

This research work has received funding from the European Union's Horizon 2020 research and innovation program under grant agreement No 864298 (project ATTEST).

References

[1] Migliavacca Gianluigi, Rossi Marco, Six Daan, Dzamarija Mario, Horsmanheimo Seppo, Madina Carlos, Kockar Ivana, Morales Juan Miguel. SmartNet: H2020 project analysing TSO-DSO interaction to enable ancillary services provision from distribution networks. CIRED-Open Access Proc J 2017;2017.

[2] Givisiez Arthur Gonçalves, Petrou Kyriacos, Ochoa Luis F. A review on TSO-DSO coordination models and solution techniques. Electr Power Syst Res 2020;189:106659.

[3] Gržanić Mirna, Capuder Tomislav, Bolfek Martin, Capitanescu Florin. A review of practical aspects of existing TSO-DSO coordination mechanisms in Europe and proposal of an innovative hybrid model in ATTEST project. In: 2021 IEEE international conference on environment and electrical engineering and 2021 IEEE industrial and commercial power systems Europe (EEEIC/I&CPS Europe). 2021, p. 1–6.

[4] Papavasiliou Anthony, Mezghani Ilyes. Coordination schemes for the integration of transmission and distribution system operations. In: IEEE-Power systems computation conference. PSCC, 2018, p. 1–7.

[5] Yuan Zhao, Hesamzadeh Mohammad Reza. Hierarchical coordination of TSO-DSO economic dispatch considering large-scale integration of distributed energy resources. Appl Energy 2017;195:600–15.

[6] Mohammadi Ali, Mehrtash Mahdi, Kargarian Amin. Diagonal quadratic approximation for decentralized collaborative TSO+DSO optimal power flow. IEEE Trans Smart Grid 2018;10(3):2358–70.

[7] Tang Kunjie, Dong Shufeng, Ma Xiang, Lv Leiyan, Song Yonghua. Chance-constrained optimal power flow of integrated transmission and distribution networks with limited information interaction. IEEE Trans Smart Grid 2020;12(1):821–33.

[8] Lin Chenhui, Wu Wenchuan, Chen Xin, Zheng Weiye. Decentralized dynamic economic dispatch for integrated transmission and active distribution networks using multi-parametric programming. IEEE Trans Smart Grid 2017;9(5).

[9] Li Zhengshuo, Sun Hongbin, Guo Qinglai, Wang Jianhui, Liu Guangyi. Generalized master-slave-splitting method and application to transmission-distribution coordinated energy management. IEEE Trans Power Syst 2018;34(6):5169–83.

[10] Bragin Mikhail, Dvorkin Yury. TSO-DSO operational planning coordination through l_1-proximal surrogate Lagrangian relaxation. IEEE Trans Power Syst 2021;37(2):1274–85.

[11] Li Zhengshuo, Xu Tong, Guo Qinglai, Sun Hongbin, Wang Jianhui. A response-function-based coordination method for transmission-distribution-coupled AC OPF. In: 2018 IEEE/PES transmission and distribution conference and exposition (T&D). IEEE; 2018, p. 1–5.

[12] Saint-Pierre Adrien, Mancarella Pierluigi. Active distribution system management: A dual-horizon scheduling framework for DSO/TSO interface under uncertainty. IEEE Trans Smart Grid 2016;8(5).

[13] Kontis Eleftherios O, del Nozal Álvaro Rodríguez, Mauricio Juan M, Demoulias Charis S. Provision of primary frequency response as ancillary service from active distribution networks to the transmission system. IEEE Trans Smart Grid 2021;12(6):4971–82.

[14] Karagiannopoulos Stavros, Mylonas Costas, Aristidou Petros, Hug Gabriela. Active distribution grids providing voltage support: The swiss case. IEEE Trans Smart Grid 2020;12.

[15] Soares Tiago, Carvalho Leonel, Morais Hugo, Bessa Ricardo J, Abreu Tiago, Lambert Eric. Reactive power provision by the DSO to the TSO considering renewable energy sources uncertainty. Sustain Energy Grids Netw 2020;22:100333.

[16] Silva João, Sumaili Jean, Bessa Ricardo J, Seca Luís, Matos Manuel A, Miranda Vladimiro, Caujolle Mathieu, Goncer Belen, Sebastian-Viana Maria. Estimating the active and reactive power flexibility area at the TSO-DSO interface. IEEE Trans Power Syst 2018.

[17] Capitanescu Florin. TSO-DSO interaction: Active distribution network power chart for TSO ancillary services provision. EPSR 2018.

[18] Kalantar-Neyestanaki Mohsen, Sossan Fabrizio, Bozorg Mokhtar, Cherkaoui Rachid. Characterizing the reserve provision capability area of active distribution networks: A linear robust optimization method. IEEE Trans Smart Grid 2019;11(3).

[19] Contreras Daniel A, Rudion Krzysztof. Computing the feasible operating region of active distribution networks: Comparison and validation of random sampling and optimal power flow based methods. IET GTD 2021;15.

[20] Capitanescu Florin. OPF integrating distribution systems flexibility for TSO real-time active power balance management. IET 2018.

[21] Marques Luciana, Sanjab Anibal, Mou Yuting, Le Cadre Hélène, Kessels Kris. Grid impact aware tso-dso market models for flexibility procurement: Coordination, pricing efficiency, and information sharing. IEEE Trans Power Syst 2022.

[22] Sun Xiaotian, Xie Haipeng, Wang Yun, Chen Chen, Bie Zhaohong. Pricing for TSO-DSO coordination: A decentralized incentive compatible approach. IEEE Trans Power Syst 2022.

[23] Pérez Néstor Rodríguez, Domingo Javier Matanza, López Gregorio López, Ávila José Pablo Chaves, Bosco Ferdinando, Croce Vincenzo, Kukk Kalle, Uslar Mathias, Madina Carlos, Santos-Mugica Maider. ICT architectures for TSO-DSO coordination and data exchange: a European perspective. IEEE Trans Smart Grid 2022.

[24] Alizadeh Mohammad Iman, Usman Muhammad, Capitanescu Florin, Madureira Andre Guimaraes. A novel TSO-DSO ancillary service procurement coordination approach for congestion management. In: 2022 IEEE power & energy society general meeting. PESGM, 2022, p. 1–5.

[25] Li Zhengshuo, Wang Jianhui, Sun Hongbin, Qiu Feng, Guo Qinglai. Robust estimation of reactive power for an active distribution system. IEEE Trans Power Syst 2019;34(5):3395–407.

[26] Pearson Simon, Wellnitz Sonja, del Granado Pedro Crespo, Hashemipour Naser. The value of TSO-DSO coordination in re-dispatch with flexible decentralized energy sources: Insights for Germany in 2030. Appl Energy 2022;326:119905.

[27] Gill Simon, Kockar Ivana, Ault Graham W. Dynamic optimal power flow for active distribution networks. IEEE Trans Power Syst 2013;29(1):121–31.

[28] Capitanescu Florin. Suppressing ineffective control actions in optimal power flow problems. IET Gener Transm Distrib 2020;14(13):2520–7.

[29] Baran Mesut E, Wu Felix F. Network reconfiguration in distribution systems for loss reduction and load balancing. IEEE Power Eng Rev 1989;9(4):101–2.

[30] Usman Muhammad, Capitanescu Florin. A stochastic multi-period AC optimal power flow for provision of flexibility services in smart grids. In: IEEE PowerTech Madrid, Spain. 2021, p. 1–6.

[31] Box George. Box and jenkins: Time series analysis, forecasting and control. In: A very British affair. Springer; 2013, p. 161–215.

[32] Dunning Iain, Huchette Joey, Lubin Miles. JuMP: A modeling language for mathematical optimization. SIAM Rev 2017;59(2).

[33] Wächter Andreas, Biegler Lorenz T. On the implementation of an interior-point filter line-search algorithm for large-scale nonlinear programming. Math Program 2006;106(1):25–57.

[34] Alizadeh Mohammad Iman, Capitanescu Florin. A tractable linearization-based approximated solution methodology to stochastic multi-period AC security-constrained optimal power flow. IEEE Trans Power Syst 2022. Accepted.

[35] Usman Muhammad, Capitanescu Florin. A novel tractable methodology to stochastic multi-period AC OPF in active distribution systems using sequential linearization algorithm. IEEE Trans Power Syst 2022.